

UC Irvine

UC Irvine Previously Published Works

Title

Viral-mimicking protein nanoparticle vaccine for eliciting anti-tumor responses

Permalink

<https://escholarship.org/uc/item/1b32k020>

Authors

Molino, Nicholas M

Neek, Medea

Tucker, Jo Anne

et al.

Publication Date

2016-04-01

DOI

10.1016/j.biomaterials.2016.01.056

Copyright Information

This work is made available under the terms of a Creative Commons Attribution-NonCommercial-NoDerivatives License, available at

<https://creativecommons.org/licenses/by-nc-nd/4.0/>

Peer reviewed



Viral-mimicking protein nanoparticle vaccine for eliciting anti-tumor responses



Nicholas M. Molino^a, Medea Neek^a, Jo Anne Tucker^b, Edward L. Nelson^{b, c, d},
Szu-Wen Wang^{a, c, e, *}

^a Department of Chemical Engineering and Materials Science, University of California, Irvine, CA 92697, USA

^b Department of Medicine, University of California, Irvine, CA 92697, USA

^c Chao Family Comprehensive Cancer Center, University of California, Irvine, CA 92697, USA

^d Institute for Immunology, University of California, Irvine, CA 92697, USA

^e Department of Biomedical Engineering, University of California, Irvine, CA 92697, USA

ARTICLE INFO

Article history:

Received 17 January 2016

Accepted 25 January 2016

Available online 1 February 2016

Keywords:

Protein nanoparticle

T cells

CD8

Biomimetic

Tumor-associated antigen

Vaccine

ABSTRACT

The immune system is a powerful resource for the eradication of cancer, but to overcome the low immunogenicity of tumor cells, a sufficiently strong CD8⁺ T cell-mediated adaptive immune response is required. Nanoparticulate biomaterials represent a potentially effective delivery system for cancer vaccines, as they can be designed to mimic viruses, which are potent inducers of cellular immunity. We have been exploring the non-viral pyruvate dehydrogenase E2 protein nanoparticle as a biomimetic platform for cancer vaccine delivery. Simultaneous conjugation of a melanoma-associated gp100 epitope and CpG to the E2 nanoparticle (CpG-gp-E2) yielded an antigen-specific increase in the CD8⁺ T cell proliferation index and IFN- γ secretion by 1.5-fold and 5-fold, respectively, compared to an unbound peptide and CpG formulation. Remarkably, a single nanoparticle immunization resulted in a 120-fold increase in the frequency of melanoma epitope-specific CD8⁺ T cells in draining lymph nodes and a 30-fold increase in the spleen, relative to free peptide with free CpG. Furthermore, in the very aggressive B16 melanoma murine tumor model, prophylactic immunization with CpG-gp-E2 delayed the onset of tumor growth by approximately 5.5 days and increased animal survival time by approximately 40%, compared to PBS-treated animals. These results show that by combining optimal particle size and simultaneous co-delivery of molecular vaccine components, antigen-specific anti-tumor immune responses can be significantly increased.

© 2016 Elsevier Ltd. All rights reserved.

1. Introduction

Recent years have brought an improved understanding of the interplay between cancer and the immune system, increasing clinical interest in immunotherapy [1]. The immune system possesses many unique advantages for targeted disease eradication [2,3], mediated primarily by robust CD8⁺ cytotoxic T lymphocyte (CTL) responses [4,5]. Strategies for therapeutic vaccination against tumor-associated antigens (TAAs) have included administration of whole protein antigen [6], mature peptide epitopes [7], cell lysate

[8], and adoptive transfer strategies [9,10]. Peptide vaccines, in particular, represent an attractive strategy by allowing for incorporation of multiple mature epitopes; however, suboptimal CTL responses are typically observed in clinical trials, prompting the need for enhanced approaches [11].

In contrast to peptide vaccines, viruses are effective inducers of CTL immunity [12]. They are generally comprised of one or a few protein monomers that self-assemble into symmetrical hollow structures packaged with genetic material [13]. Dendritic cells (DCs), perhaps the most potent antigen presenting cell (APC) for induction of adaptive immunity, have evolved sensing mechanisms (e.g., Toll-like receptors; TLRs) to recognize common features of pathogens (e.g., viruses) for activation and orchestration of CTL responses [14]. In addition, DCs are effective cross-presenters of exogenous antigens, such as those of viruses and

* Corresponding author. Department of Chemical Engineering and Materials Science, University of California, Irvine, 916 Engineering Tower, Irvine, CA 92697-2575, USA.

E-mail address: wangsw@uci.edu (S.-W. Wang).

cancers [15]. Therefore, mirroring the pathogenic features of viruses, sans virulence, with biomaterials represents a potentially effective approach of delivering TAA-derived epitopes [13]. While active targeting of DCs with biomaterials is an approach with demonstrated potential [16], an advantage of virus mimicry is the passive targeting and preferential accumulation within immunologically rich regions (*i.e.* lymph nodes) and interaction with DCs following immunization [17].

In particular, the viral size, repetitive structural features, and co-delivery of immune-inducing viral components are characteristics that have been attributed to the induction of an effective immune response [17]. The weak immune responses to peptide (and protein) TAA vaccines may be related to physical size, in which these components are typically well below the size range reported to be optimal for efficient delivery to APCs [17]. Cancer vaccine delivery vehicles such as synthetic nanostructured biomaterials (*e.g.*, liposomes, metals, and polymers) and natural systems (*e.g.*, viruses and exosomes) have been explored [18–20] as alternatives to traditional TAA peptide delivery platforms to enhance the efficacy of the anti-tumor immune response.

Since the first clinically approved virus-like particle (VLP)-based vaccine (Gardasil), many other nanoparticulate protein-based assemblies have been clinically developed as vaccines, primarily for infectious diseases [13,21], and in particular for induction of adaptive T cell responses. For example, VLP-based vaccines targeting influenza were previously shown to induce protective CD8⁺ T cell responses following a single immunization [22]. In cancer therapy, Q β VLPs have been undergoing clinical trials for vaccination against the Melan-A/MART1 melanoma-associated tumor antigen [23]. Autologous tumor-derived heat shock proteins, hypothesized to bind autologous TAAs, have been explored for cancer vaccination as well, supporting clinical interest in natural protein-derived nanoassemblies that carry antigens [24,25].

In this work, we examine the use of the E2 subunit of pyruvate dehydrogenase for cancer immunotherapy applications. The E2 nanoparticle is a self-assembling hollow protein cage with an approximately 30-nm diameter and high physical stability [26]. It is also of non-viral origin and has been shown to be amenable to functionalization in biomedical applications [26–29]. Our research group has previously demonstrated significantly enhanced activation and cross-presentation of a model antigen using the E2 nanoparticle for delivery to and activation of DCs [30]. This increased activation, mediated by virus-mimicking E2 nanoparticles, may allow the immune system to overcome the low immunogenicity or tolerance to tumor antigens. Based on this prior study with ovalbumin, we hypothesized that E2-mediated co-delivery of a repetitive TAA epitope, together with CpG packaged for endolysosomal release, would induce increased antigen-specific anti-tumor responses following immunization (relative to other tumor peptide vaccine formulations of the same epitope).

Our target epitope in this current work is the gp100 melanocyte differentiation protein, a TAA that is a tumor regression antigen and a clinically-pursued target in humans [31]. The antigen is highly conserved between human and mouse, enabling testing of human vaccines in a murine model [5]. While the full gp100 protein has been loaded to heat-shock proteins for vaccination in murine melanoma models [32], to our knowledge, clinically-applicable gp100 epitopes packaged with DC activators have not been previously tested using non-viral protein nanoparticle systems. This study examines the induction of CD8⁺ T cell and anti-tumor responses that are specific to a gp100 peptide epitope and demonstrates that the viral-mimicking E2 nanoparticle platform may be a particularly effective delivery system for tumor antigens.

2. Methods

2.1. Materials

All buffer reagents were purchased from Fisher Scientific, unless otherwise noted. The oligodeoxynucleotide TLR9 ligand CpG 1826 (5'-tccatgacgttctgacgtt-3') (CpG) was synthesized with a phosphorothioated backbone and 5' benzaldehyde modification by TriLink Biotechnologies. The KVPRNQDWL peptide (gp100₂₅₋₃₃, herein abbreviated as “gp100”) was from Genscript, and the custom gp100 peptide (for conjugation to E2) was synthesized with an N-terminal cysteine by Thinkpeptides (Proimmune). Unless otherwise noted, cell culture media was comprised of RPMI 1640 (Mediatech) supplemented with 10% heat-inactivated fetal bovine serum (Hyclone), 1 mM sodium pyruvate (Hyclone), 2 mM L-glutamine (Lonza), 100 units/ml penicillin (Hyclone), 100 μ g/ml streptomycin (Hyclone), 50 μ M 2-mercaptoethanol (Sigma), and 0.1 mM non-essential amino acids (Lonza) (complete RPMI media). Carboxy-fluorescein diacetate succinimidyl ester (CFSE), flow cytometry antibodies, and recombinant murine GM-CSF were purchased from eBioscience. Phytohemagglutinin (PHA-M) was from Gibco.

2.2. Mice and cell lines

All animal studies were carried out in accordance with protocols approved by the Institute for Animal Care and Use Committee (IACUC) at the University of California, Irvine. Female C57BL/6 mice and pmel-1 mice, which display transgenic T-cell receptors specific for the gp100₂₅₋₃₃ epitope in the context of H2-D^b in a C57BL/6 background [5], were purchased from Jackson Laboratories and used at 6–12 weeks of age, unless otherwise noted. The B16-F10 murine melanoma cell line was purchased from ATCC and cultured in DMEM media supplemented with 10% FBS according to vendor instructions.

2.3. E2 purification and characterization

The D381C E2 protein nanoparticle (E2) was prepared and characterized as previously described [26,30]. D381C is an E2 mutant with a non-native cysteine introduced to the internal cavity of the nanoparticle at amino acid location 381 for site-specific conjugation. Briefly, proteins were expressed in *E. coli* and soluble cell lysates were applied to a HiPrep Q Sepharose anion exchange column (GE Healthcare) followed by a Superose 6 size exclusion column (GE Healthcare) for purification. The hydrodynamic diameter of the purified proteins was analyzed by dynamic light scattering (DLS; Zetasizer Nano ZS, Malvern). Electrospray ionization mass spectrometry and SDS-PAGE confirmed molecular weight and purity. Final protein preparations were stored in 50 mM potassium phosphate at pH 7.4 with 100 mM NaCl (phosphate buffer) at 4 °C for short-term and –80 °C for long-term storage. Residual LPS was removed using Triton X-114, and endotoxin levels were checked as previously described [30].

2.4. CpG and gp100 conjugation

Aldehyde-terminated CpG oligonucleotides were covalently packaged within E2, and cysteine-terminated peptide epitopes were displayed on the external surface of E2 as previously described [30]. Briefly, the cysteines in the E2 internal cavity were reduced with TCEP (Pierce), followed by incubation with N-(β -maleimidopropionic acid) hydrazide (BMPH) linker (Pierce) and removal of unreacted linker. Conjugation with the aldehyde-modified CpG 1826 involved overnight incubation and excess CpG removal. The number of conjugated CpG molecules was

determined previously to average 22 CpG molecules per E2 particle [30]; this conjugation ratio was kept constant throughout this study.

For peptide attachment, peptide was added to SMCC-functionalized E2 at a 10-fold excess to E2 monomer. The negative control consisted of water (solvent for SMCC) combined with E2 in the initial reaction step, and reactions were otherwise carried out as described previously [30]. For measurement of peptide conjugation ratios, gp100-conjugated E2 (gp-E2) was analyzed by high performance liquid chromatography (HPLC, Shimadzu) with a Zorbex C18 column using a water:acetonitrile gradient. Mixtures were examined by HPLC, and the remaining unconjugated peptide was quantified with a standard curve of free cysteine-terminated gp100 peptide. The difference between gp-E2 and negative control reactions determined the number of conjugated peptides per nanoparticle.

DLS was used to measure hydrodynamic diameters, and transmission electron micrographs of 2% uranyl acetate-stained nanoparticle on Cu 150 mesh Formvar-carbon coated grids were obtained on a JEM1200EX (JEOL) with a Bioscan600W digital camera (Gatan) [26,30].

2.5. Bone marrow-derived dendritic cells

Bone marrow-derived DCs (BMDCs) were generated as previously described [30]. Briefly, red blood cell (RBC)-depleted C57BL/6 bone marrow cells were plated at 2×10^5 cells/ml (10 ml total) on sterile bacteriological Petri dishes (Fisher) in complete RPMI media supplemented with 20 ng/ml murine recombinant GM-CSF. Cells were maintained at 37 °C and 5% CO₂, and 10 ml fresh complete RPMI with 20 ng/ml GM-CSF was added on day 3. On day 6, 50% of the media was replaced, and the non-adherent cells were pelleted and added back to the plates. Loosely and non-adherent cells were collected and used as immature BMDCs on day 8.

2.6. T cell proliferation and IFN- γ secretion assays

BMDCs (5×10^3 cells/well in 96-well plate) were incubated in complete RPMI media with various combinations of vaccine elements, either as individual free elements or conjugated to E2 (Table 1). After 4 h, wells were washed twice with PBS to remove excess antigen, free CpG, and/or E2, with fresh complete RPMI added thereafter. We evaluated multiple gp100 peptide epitope concentrations (10, 100, or 1000 nM); the peptide concentration was maintained whether free or conjugated to E2. Similarly, the concentration of CpG oligonucleotide was kept constant between formulations. The amount of CpG packaged within the E2 nanoparticles was previously determined to be approximately 10% w/w to E2 (i.e. 5 μ g CpG per 50 μ g E2) [30], and unconjugated, free CpG control concentrations were based on this number.

To isolate CD8⁺ T cells, the spleens and lymph nodes from pmel-1 mice were crushed through a 70- μ m cell strainer in ice cold PBS and centrifuged at 300 \times g for 5 min. RBCs were depleted with ACK

lysing buffer and the cells were applied to the EasySep CD8 T cell negative isolation kit from STEMCELL according to the manufacturer's instructions.

Briefly, for T cell proliferation assays, CD8⁺ T cells were suspended at 2×10^7 cells/ml in PBS, diluted with an equal volume of PBS containing 5 μ M of the intracellular dye CFSE (1×10^7 cells/ml and 2.5 μ M CFSE final), and incubated at room temperature for 10 min. The reaction was quenched by 10-fold dilution in 37 °C RPMI containing 10% FBS and cells were washed an additional time with PBS. Freshly prepared CFSE-labeled pmel-1 CD8⁺ T cells were added to the antigen-pulsed BMDCs at 5×10^4 cells/well (10:1 T cells:DCs) and cultured at 37 °C for 72 h. Negative control wells consisted of co-culture without any antigen stimulation and positive control included α CD3/ α CD28 Dynabeads (Gibco) added at a 1:1 ratio with T cells. Cells were harvested, stained with APC-tagged anti-CD8, and analyzed by an Accuri C6 flow cytometer for CFSE dilution of CD8⁺ cells. Proliferation index (PI), a measure of cell division, was calculated as

$$PI = \frac{\sum_0^i N_i}{\sum_0^i \frac{N_i}{2^i}}$$

where i is the number of divisions and N is the number of cells within that division [33].

For IFN- γ secretion measurements, culture supernatants were collected prior to cell collection for proliferation assays and assayed with the Mouse IFN- γ ELISA Ready-Set-Go kit (eBioscience), following the manufacturer's instructions. Data is reported as IFN- γ concentration relative to concentration obtained for BMDCs pulsed with free gp100 peptide alone.

2.7. IFN- γ ELISpot & CTL lysis assays

Mice (C57BL/6) were subcutaneously immunized with 100 μ l formulations containing 5 μ g each of gp100 peptide and CpG in PBS (either free or E2-bound; equivalent to 50 μ g of E2-based nanoparticle formulations) bilaterally at the base of the tail. After 7 days, single cell suspensions were prepared from the spleen and draining lymph nodes (inguinal, axillary, brachial, and iliac). Isolated splenocyte and lymph node cells were analyzed by flow cytometry to determine the percentages of various cell types present following immunization. Cells were stained in PBS + 1% BSA for 30 min on ice with antibodies against CD11c, F4/80, B220, CD3, CD4, CD8, PD-1, and (intracellular) FoxP3. RBCs were depleted from splenocytes with ACK lysing buffer.

For IFN- γ ELISpot, cells were resuspended in complete RPMI and added at 4×10^5 and 8×10^5 cells/well to ELISpot plates (PVDF membrane 96-well plates, Millipore), pre-coated overnight with anti-mouse IFN- γ antibody from the Mouse IFN- γ ELISpot Ready-Set-Go kit (eBioscience). Cells were incubated for 24 h at 37 °C with either 10 μ g/ml (~10 μ M) gp100 peptide or irrelevant peptide (ovalbumin peptide, SIINFEKL). Negative control consisted of media only and positive control wells contained 1.5% PHA-M. Spots were developed according to the kit manufacturer's protocol and were detected and analyzed by the Cellular Technology Ltd. ELISpot reader and Immunospot Analysis Pack software, respectively.

To examine the specific lysis of cells bearing the gp100 TAA, splenocytes were cultured in complete RPMI at 5×10^6 cells/ml with 10 μ g/ml free gp100 for 24 h, washed twice with PBS to remove unbound peptide, and cultured in fresh complete RPMI for an additional 48 h. B16-F10 melanoma cells (H-2D^b and gp100⁺) were plated at 5×10^3 cell/well in a round-bottom 96 well tissue culture-treated plate along with the gp100-stimulated splenocytes at a 50:1 effector-to-target ratio. Cytotoxicity was measured by

Table 1

List of various gp100 formulations used in this study and their respective abbreviations (gp100 peptide sequence: KVPRNQDWL).

Formulation	Label
Free peptide (gp100 ₂₅₋₃₃)	gp100
Free peptide + Free CpG	gp100 + CpG
Free peptide + Free CpG + Free E2	gp100 + CpG + E2
Free peptide + CpG-conjugated E2	gp100 + CpG-E2
Peptide-conjugated E2 + Free CpG	gp-E2 + CpG
Peptide and CpG simultaneously conjugated to E2	CpG-gp-E2

lactate dehydrogenase release with the CytoTox 96 non-radioactive cytotoxicity assay (Promega) following the manufacturer's instructions. Data is reported as % lysis, calculated as:

$$\% \text{ Lysis} = \frac{(\text{coculture LDH release}) - (\text{background LDH release})}{(\text{maximum B16 LDH release}) - (\text{background B16 LDH release})} \times 100,$$

where "background LDH release" is the sum of LDH release from B16-F10 and splenocyte cells each cultured alone, and "maximum B16 LDH release" is from lysed B16-F10 cells using lysis buffer from the kit.

2.8. Tumor challenge

C57BL/6 mice (6–10 week) were immunized subcutaneously, bilaterally at the base of the tail with 50 μg CpG-gp-E2 in 100 μl PBS or with an equivalent volume of PBS on days –28 and –14 ($n = 5$ per treatment group). On day 0, 1×10^5 B16-F10 melanoma cells were subcutaneously inoculated in the right flank, and tumor size was measured daily with a caliper. Tumor volume was calculated as $(0.5 \times \text{shortest diameter}^2 \times \text{longest diameter})$ and mice were sacrificed when tumor volumes reached 500 mm^3 .

2.9. Statistical analysis

For *in vitro* and *ex vivo* studies, statistical analyses were carried out using Microsoft Excel and GraphPad Prism. Data is reported as mean \pm standard error of the mean (S.E.M.) of at least three independent experiments (unless otherwise noted), with each data point from an independent experiment resulting from duplicate measurements for each *in vitro* experiment and triplicate measurements for each experiment requiring immunization. Statistical significance was determined by performing a one-way analysis of variance (ANOVA) followed by a Dunnett's test, comparing formulations to the viral-mimicking CpG-gp-E2 protein nanoparticle (hypothesized to induce the highest immune response, based on prior results [30]), unless otherwise noted. P-values less than 0.05 were considered significant.

Statistical analyses for *in vivo* survival curves were carried out using the log-rank (Mantel–Cox) test in GraphPad Prism. Data presented are representative of two independent experiments, with five mice per treatment group ($n = 5$) in each independent experiment. The elapsed time to the onset of palpable tumors for the different treatment groups were compared using a two-tailed Student's t-test, assuming unequal variances. P-values less than 0.05 were considered significant.

3. Results and discussion

3.1. Conjugation of CpG and gp100 peptide to E2 yields intact nanoparticles

CpG and gp100 peptides were successfully conjugated to the E2 nanoparticle, and the results are consistent with those previously published for conjugation of an ovalbumin peptide epitope (Fig. 1A) [30]. The gp-E2 nanoparticle displayed a broad band on SDS-PAGE in the molecular weight range of 30–35 kDa, consistent with conjugation of multiple gp100 peptides (with linker) that each add 1592 Da to the E2 monomer (which is 28105 Da). These comparable results between different peptides demonstrate the ability to

successfully employ the same conjugation strategy [30]. CpG attached to the internal E2 cysteine at site 381 yielded two distinct bands, one at 28 kDa (28105 Da for unconjugated E2 monomer and

28288 for E2 monomer with linker) and one at 35 kDa (34879 Da for E2 with CpG). Our previous study quantified this covalent encapsulation to be 22 ± 3 CpG per E2 nanoparticle or ~10% w/w (CpG-E2) [30]. CpG molecules are released from E2 under acidic endolysosomal conditions, and the CpG-E2 particle facilitated enhanced DC uptake and activation, compared to free CpG [30].

Simultaneous attachment of both CpG (internally) and gp100 peptide (externally) to the E2 monomers was also confirmed. Two distinct broad bands in the molecular weight ranges of 30–35 kDa (gp-E2) and 35–40 kDa (CpG-gp-E2) were observed (last lane of Fig. 1A). HPLC analysis revealed that gp100 was linked to the E2 nanoparticle surface at a ratio of 3.9 ± 0.6 peptides/monomer or ~10% w/w (234 ± 36 peptides/nanoparticle), greater than what we observed for the ovalbumin peptide [30].

DLS measurements ($n = 3$) of the gp-E2 and CpG-gp-E2 nanoparticles measured a hydrodynamic diameter of 31.6 ± 1.3 nm and 30.2 ± 0.7 nm, respectively, consistent with short peptides attached on the surface of an intact E2 core (Fig. 1B). TEM analysis further confirmed intact non-aggregated CpG-gp-E2 nanoparticles (Fig. 1C) that are within the reported optimal range for viral-based vaccines [17]. These nanoparticle diameters are also consistent with sizes observed for our conjugation with other peptides and guest molecules [26,29,30,34], further demonstrating the versatility of the E2 platform for attachment of various molecules (e.g., epitopes).

3.2. E2 co-delivery of gp100 and CpG increases CD8⁺ T cell IFN- γ secretion *in vitro*

The CpG-gp-E2 nanoparticle increased CD8⁺ T cell-specific IFN- γ secretion *in vitro*, compared to other formulations (Fig. 2). There was a statistically significant increase in relative CD8⁺ T cell IFN- γ secretion over other formulation groups, when CD8⁺ T cells from pmel-1 mice were co-cultured with BMDCs loaded with the CpG-gp-E2 nanoparticle at both 100 nM and 1000 nM of gp100. While differences between groups at 10 nM gp100 were not significant ($p > 0.05$), the trend was similar between the formulations, with the CpG-gp-E2 formulation exhibiting the highest average level of IFN- γ (Fig. S1). We also observed a dose response of cytokine secretion, where increasing CpG-gp-E2 concentrations corresponded to an increase in IFN- γ levels (20 ± 10 , 300 ± 70 , and 11000 ± 4000 pg/mL for 10, 100, and 1000 nM of gp100, respectively).

Viral infections are accompanied by increased Type II interferon (i.e. IFN- γ) [35], a cytokine that supports the effector functions of CTL and is believed to be critical for anti-cancer immunity and tumor suppression [36]. More specifically, IFN- γ has been shown to play a key role in gp100-positive melanoma sensitization to the lytic activity of CTL [37]. Our results indicate that the combination of a gp100 peptide epitope and CpG within the viral-mimicking E2 platform enhances the ability to induce *in vitro* antigen-specific IFN- γ secretion. Similar results have been observed with other polymeric nanoparticle systems *in vitro* as well, delivering a TLR4 agonist and gp100 epitopes, where anti-tumor responses were observed *in vivo*

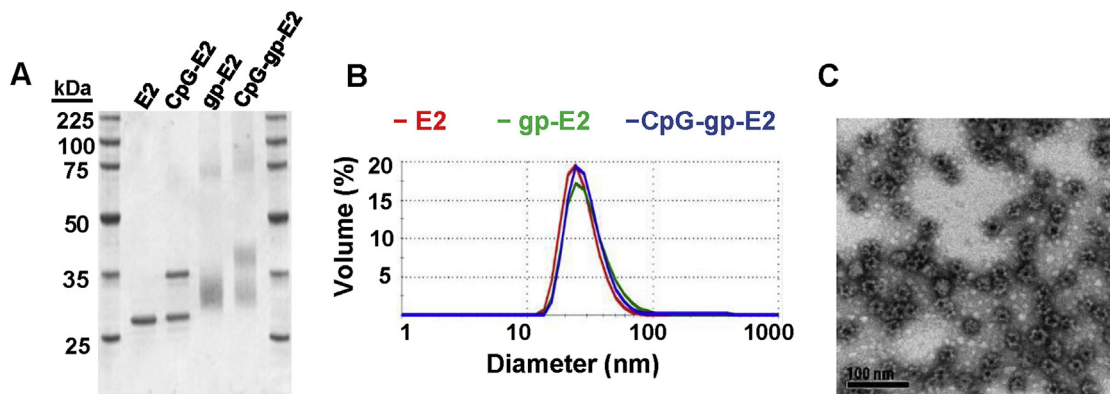


Fig. 1. Physicochemical characterization of functionalized nanoparticles. A) Functionalization of the E2 nanoparticle (E2; 28105 Da monomer) with the CKVPRNQDWL peptide (gp-E2) shows a broad band in the 30–35 kDa range, supporting heterogeneous conjugation of the gp100 peptide to the external E2 lysines. Simultaneous conjugation of gp100 peptide and CpG (lane CpG-gp-E2) shows two distinct broad signals in the 30–35 kDa and 35–40 kDa range. B) Representative DLS data reveal nanoparticle sizes within the optimal reported vaccine size range. C) Transmission electron micrograph of CpG-gp-E2 stained with 2% uranyl acetate confirms monodisperse, intact nanoparticles. Scale bar is 100 nm.

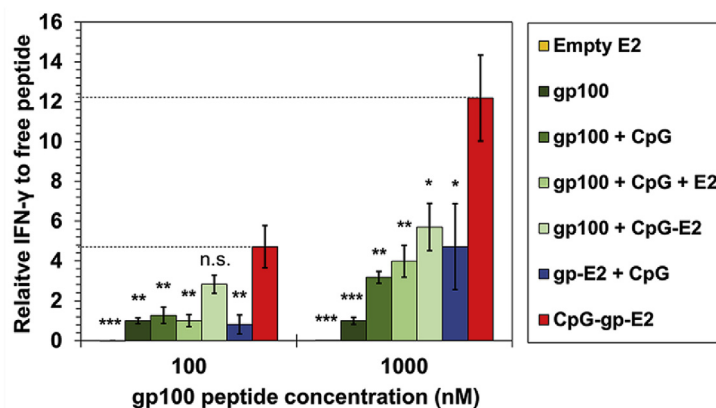


Fig. 2. Pmel-1 CD8⁺ T cells show increased antigen-specific IFN- γ secretion when stimulated by BMDCs loaded with the CpG-gp-E2 nanoparticle, compared to other formulations. IFN- γ levels measured with ELISA were normalized to the free gp100 peptide formulation (gp100) as baseline. Data are presented as mean \pm S.E.M. (n = 3) and were analyzed using a one-way ANOVA followed by Dunnett's test comparing all means to CpG-gp-E2 within each concentration (*p < 0.05; **p < 0.01; ***p < 0.001).

[38]. Therefore, our ability to drive increased antigen-specific IFN- γ secretion demonstrates the potential superiority of the E2 nanoparticle as a viral-mimicking melanoma peptide vaccine delivery platform, compared to more conventional clinical trial formulations (i.e. free gp100 peptide mixed with free CpG).

3.3. E2 co-delivery of gp100 and CpG increases DC-mediated CD8⁺ T cell proliferation

Simultaneous conjugation of CpG (internally) and gp100 (externally) to the E2 nanoparticle resulted in increased DC-mediated CD8⁺ T cell proliferation. We observed a significant increase in pmel-1 CD8⁺ T cell proliferation over 72 h in response to the CpG-gp-E2 formulation, where we were able to detect up to ~7 divisions, compared to all other formulations at the 100 nM peptide concentration level (Fig. 3). The CpG-gp-E2 nanoparticle formulation induced a stronger proliferative response, with a greater proportion of CD8⁺ T cells observed in later divisions (Fig. 3A), quantified by proliferation index (PI) (Fig. 3B). In contrast to our IFN- γ ELISA results (Fig. 2), the average CD8⁺ T cell PI did not increase at higher antigen concentrations in the CpG-gp-E2 nanoparticle formulation (Fig. S2); in fact, statistically-significant differences in relative PI between groups was observed only at 100 nM gp100. This data supports the possibility of antigen-specific

T cell dysfunction, exhaustion/overstimulation, and/or deletion at high antigen doses [39], and suggests that there are optimal concentrations of the vaccine components (i.e. peptide and CpG), with respect to CD8⁺ T cell proliferation, when packaged simultaneously in the viral-mimicking E2.

3.4. E2 delivery of CpG increases antigen presenting cell (APC) numbers in secondary lymphoid organs

A single immunization containing 5 μ g CpG in the E2-bound formulations (Table 1) resulted in an increase in the number of APCs (responsible for antigen processing and activation of adaptive T cell responses), including DCs, macrophages, and B cells in secondary lymphoid tissues (Fig. 4). It is known that CpG induces proliferation of B cells in mice [40], and it is likely that E2 is mediating more efficient delivery of the CpG activators to these cells as compared to free CpG. While lymphocytes such as B and T cells undergo rapid expansion *in situ* within secondary lymphoid organs following activation, APCs such as DCs and macrophages are not currently known to proliferate at such rapid rates within these organs. Recruitment or infiltration following expansion outside of secondary lymphoid organs may explain the increase in CD11c⁺ cells (primarily DCs) and F4/80⁺ cells (macrophages and Langerhans DCs), as cytokine signaling can induce increases in systemic DC numbers [41].

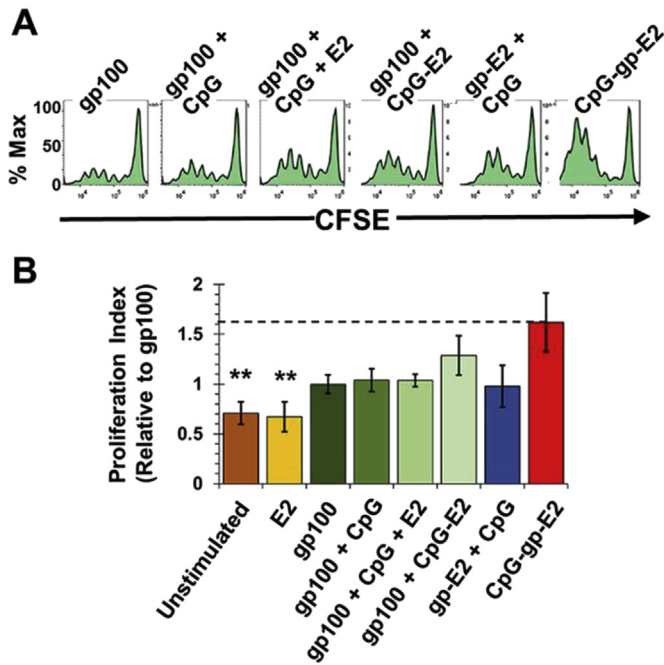


Fig. 3. Pmel-1 CD8⁺ T cells exhibit increased proliferative capacity when cultured in the presence of BMDCs loaded with the CpG-gp-E2 nanoparticle, compared to other gp100 formulations (100 nM gp100 peptide, either free or E2-bound). (A) Representative flow cytometry histograms of CFSE-labeled CD8⁺ T cells show increased proliferation in the CpG-gp-E2 group. (B) The CpG-gp-E2 nanoparticle induced the greatest CTL proliferative capacity. Data represents mean proliferation index (PI) ± S.E.M. (n = 3) and is normalized to the free gp100 peptide formulation. Statistical analysis used a one-way ANOVA followed by Dunnett's test comparing all groups to CpG-gp-E2 (**p < 0.01).

Interestingly, only the free gp100 + CpG-E2 formulation demonstrated significant increases in T cells (predominantly CD4⁺) in the draining lymph nodes (dLNs) and spleen. This observation may be partially explained by homeostatic proliferation [42] induced by TLR9-expressing, IL-7 producing cells of the lymphatics [43,44]. Elevated levels of CD8⁺ T cells in mice immunized with free gp100 + CpG-E2 may result from non-antigen-specific proliferation, whereby the T cells are not directed to exit the lymphatics [45]. The high affinity CTL epitopes on the CpG-gp-E2 virus-mimicking nanoparticle may mediate, *via* APCs, a cytokine environment less conducive to homeostatic CD4⁺ T cell proliferation and more favorable for the activation of antigen-specific CD8⁺ T cells within the dLN and spleen [12]. The departure of these antigen-specific CTL to the periphery, which happens during the first week of cell-mediated immunity to viral infection [46], may explain the apparent lack of elevated CD8⁺ T cell numbers in the secondary lymphoid organs of mice immunized with CpG-gp-E2. This absence of large increases in CD8⁺ T cell numbers in the dLN and spleen in response to CpG-gp-E2, relative to gp100 + CpG-E2 immunization, is not likely due to induction of FoxP3-expressing regulatory CD4⁺ T cells (Fig. S3), or increased exhaustion over other tested formulations, at least as measured by PD-1 expression (Fig. S4). Some level of increased PD-1 expression by CD8⁺ T cells, in response to any formulation tested (as seen in Fig. S4), is expected with homeostasis and the development of central memory, following an acute response [47].

3.5. A single immunization with CpG-gp-E2 increases antigen-specific CD8⁺ T cells

Immunization with CpG-gp-E2 nanoparticles resulted in increased frequencies of gp100-specific IFN- γ -producing CD8⁺ T

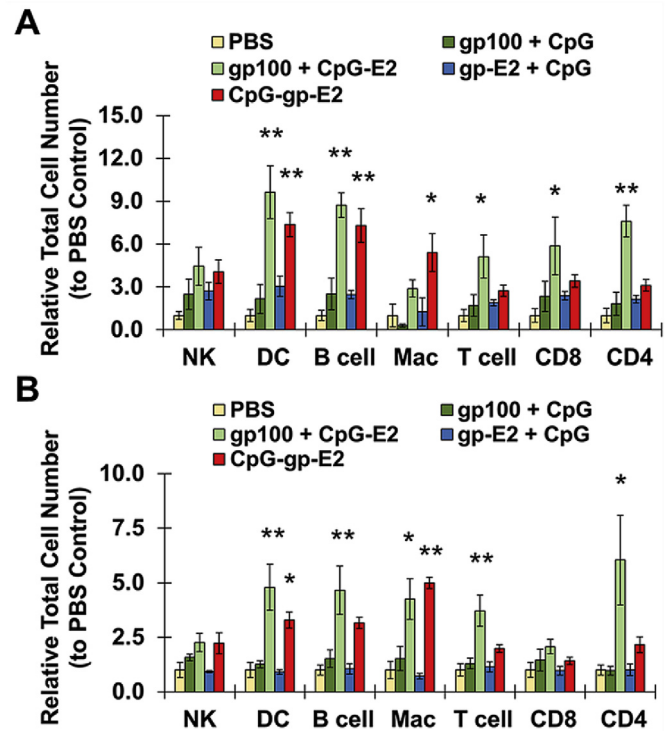


Fig. 4. Mice immunized with CpG-gp-E2 and gp100 + CpG-E2 formulations exhibited increased secondary lymphoid organ antigen presenting cell numbers in the A) draining lymph nodes and B) spleens. Vaccine formulations with antigen contained 5 μ g each of gp100 peptide and CpG ODN (either free or E2-bound). Cells measured in the secondary lymphoid organs included natural killer cells (NK), dendritic cells (DC), B cells, macrophages (Mac), T cells, CD8⁺ T cells, and CD4⁺ T cells. Data is presented as average \pm S.E.M. total cell numbers relative to the PBS control of at least 3 independent experiments. Statistical significance was determined by one-way ANOVA followed by a post hoc Tukey's test, with a pairwise comparison of all statistical means. *p < 0.05; **p < 0.01 compared to the PBS background control.

cells, as compared to other formulations of the peptide vaccine components (Fig. 5). We observed large increases in the number of gp100 peptide-specific spots in the IFN- γ ELISpot analysis of dLN cells (Fig. 5A) and splenocytes (Fig. 5B) from mice that received a single immunization with the CpG-gp-E2 viral-mimicking antigen formulation compared to all other formulations (either free or E2-bound peptide), with the exception of gp100 + CpG-E2 in the dLNs. In fact, frequencies of epitope-specific CD8⁺ T cells due to CpG-gp-E2 were 30-fold and 120-fold higher in spleen and dLNs, respectively, relative to numbers from free gp100 with free CpG. Additionally, the lack of spots observed for cells pulsed with the SIINFEKL ovalbumin epitope confirmed that the immune response was specific to gp100, rather than non-specific activation. We observed spot frequencies among total cells that were comparable to previously reported nanoparticle formulations delivering the gp100 epitope [32]. However, when compared to this previous report, we observed the expansion of gp100-specific CD8⁺ T cells following only a single injection, rather than multiple immunizations. Our IFN- γ ELISpot frequencies are also similar to previous reports using nanoparticle formulations for melanoma-specific TAAs (other than gp100) and which also demonstrated strong anti-tumor activity [38,48,49].

Interestingly, the gp100 + CpG-E2 nanoparticle formulation exhibited similar spot frequencies to CpG-gp-E2 within the dLN, implying that packaging CpG within the E2 nanoparticle enhanced local APC activation and antigen presentation and CD8⁺ T cell

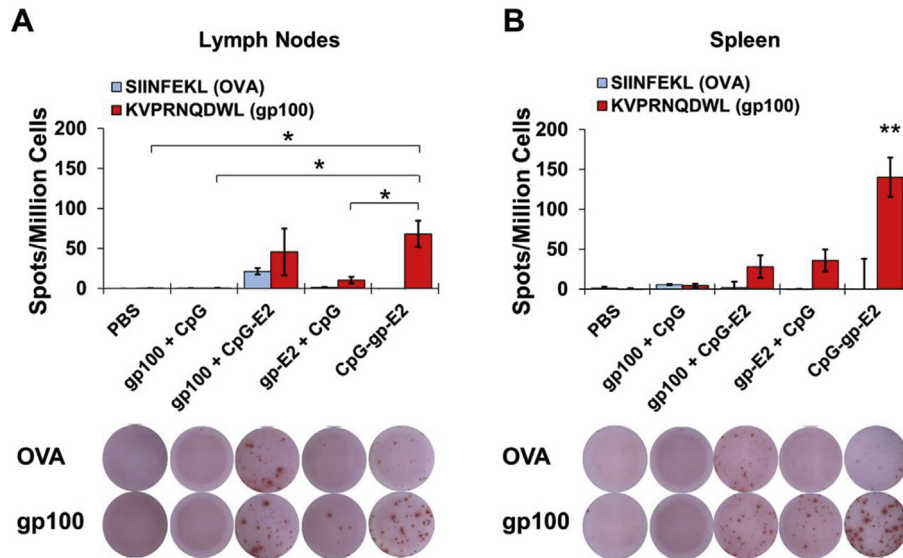


Fig. 5. Immunization with the CpG-gp-E2 nanoparticle increased the gp100-specific CTL response. Cells were isolated from the A) draining lymph nodes and B) spleens of mice immunized with different formulations (5 μ g gp100 peptide and 5 μ g CpG; unbound or bound to E2) and were cultured *ex vivo* in the presence of KVPRNQDWL peptide (gp100) or irrelevant SIINFEKL peptide (OVA) and analyzed for IFN- γ -secreting cells by ELISpot. The lower panels show representative wells from the immunization groups for negative control irrelevant peptide (OVA) and tumor antigen peptide (gp100). Data is presented as average \pm S.E.M. spots per million cells from at least 3 independent experiments. Statistical significance was determined by ANOVA followed by Dunnett's test, comparing all means to CpG-gp-E2 (* p < 0.05; ** p < 0.01).

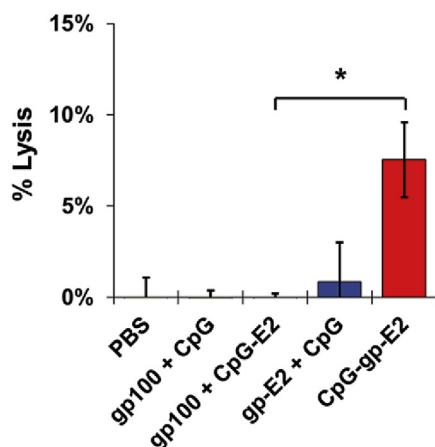


Fig. 6. Splenocytes from mice receiving a single immunization of the CpG-gp-E2 (50 μ g) nanoparticle formulation exhibited enhanced lytic ability toward B16-F10 melanoma cells (measured by release of lactate dehydrogenase). Data is presented as average \pm S.E.M. % lysis of at least 3 independent experiments. Statistical significance was determined by ANOVA followed by Dunnett's test, comparing all means to CpG-gp-E2 (* p < 0.05).

activation, even with unbound peptide. This local effect on APCs may help explain the observed non-specific IFN- γ secretion from splenocytes and dLN cells of mice immunized with the gp100 + CpG-E2 formulation.

The increased number of gp100-specific spots in the spleen compared to the dLNs from mice immunized with the CpG-gp-E2 formulation may be a result of the kinetics following a virus-induced immune response, where lymphocytes in the initial dLNs are known to respond earlier than those in the spleen [50]. It is entirely possible that CD8⁺ T cell expansion peaked in the lymph nodes and started to decline prior to our analyses, as CD8⁺ T cells may have already exited the lymph nodes or have begun contraction into the memory pool. Although of some interest, the extensive pharmacokinetic experiments and animal resources necessary to

definitively test this possibility are not warranted at this stage of development of the E2 platform.

3.6. CpG-gp-E2 immunization enhances lytic capacity of CD8⁺ T cells

CpG-containing E2 nanoparticles co-delivering surface-bound gp100 epitopes induce increased TAA-specific lysis of syngeneic tumor cells (Fig. 6). Splenocytes from CpG-gp-E2-immunized animals had greater lytic activity toward the gp100⁺ metastatic melanoma B16-F10 cell line, relative to other formulations. This CpG-gp-E2 formulation gave statistically significant increased lysis of the B16-F10 melanoma cells at a 50:1 effector-to-target ratio over the gp100 + CpG-E2 control formulation. Pairwise comparisons of the gp100 + CpG-E2 control formulation with all the remaining formulations did not exhibit any statistical differences.

Lysis of the gp100-expressing B16 cell line is an important observation, as this particular melanoma is known to exhibit low immunogenicity [51,52]. Similarly, while immunogenicity may be low for the gp100 TAA, it is an effective immunotherapeutic target antigen in humans, and therefore an attractive vaccine target [31]. Further, gp100 is a self-antigen; therefore our results indicate that we have broken central tolerance to this antigen with a single immunization of a virus-mimicking biomaterial platform. With antigens such as gp100, the formulation of the antigen or the immunotherapeutic approach is particularly critical to the successful elicitation of anti-tumor immune responses [51].

These results are consistent with our ELISpot (Fig. 5) and *in vitro* pmel-1 assays (Figs. 2 and 3) that demonstrate APC-mediated increased gp100-specific CD8⁺ T cell activation in response to the CpG-gp-E2 nanoparticle formulation. Importantly, with a single immunization, we are able to overcome tolerance and achieve specific lysis of the gp100⁺ melanoma cells at levels comparable to that of previously reported heat shock protein complexes that were given as an immunization followed by a booster (*i.e.*, 2 immunizations vs. our single immunization) [32]. This supports the

importance and advantage of simultaneous packaging of TAA epitope with danger-signal molecules (e.g., CpG). Q β VLP-mediated delivery of antigens with CpG demonstrated strong CTL responses against MHC I-restricted epitopes [53], and these particles are undergoing clinical trials as an immunotherapy for melanoma in humans [23,54], validating the potential of viral mimicry in cancer immunotherapies. Remarkably, we have achieved comparable antigen specific immune activity without the use of attenuated viruses and with a single administration.

3.7. CpG-gp-E2 immunization delays tumor growth

Based on the *in vitro* and *ex vivo* data described above, we examined the therapeutic effects of the CpG-gp-E2 nanoparticle immunization in mice challenged with B16-F10 melanoma tumor cells. Our data shows that immunization with the CpG-gp-E2 nanoparticle formulation significantly delayed tumor growth onset (15.0 ± 3.0 days), compared to PBS-treated mice (9.4 ± 0.9 days; $p < 0.05$). Tumor growth kinetic profiles further demonstrate slower tumor progression in mice immunized with CpG-gp-E2 (Fig. 7A), which exhibited a median survival time of 18 days (Fig. 7B), significantly greater than the PBS-treated median survival time of 13 days ($p < 0.002$).

Our observed B16-F10 tumor growth kinetics following prophylactic immunization with CpG-gp-E2 are similar to those reported for PLGA and heat shock protein nanoparticle immunotherapy studies delivering gp100 antigen/epitopes [32,38]. However, one major difference in our vaccination regimen, compared to these previous studies, is our schedule of a prime immunization followed by a single booster, in contrast to the two boosters administered in these previous reports [32,38]. In fact, a prime plus single booster of the heat shock protein did not demonstrate the same protective capacity compared to our single booster regimen of CpG-gp-E2, further demonstrating the advantage of our approach to deliver antigen and immune activator simultaneously in a viral-mimicking format [32]. Our anti-tumor observations support the concept that the increased antigen-specific CD8⁺ T cell numbers (Fig. 5) and induction of antigen specific *in vitro* lytic activity (Fig. 6) following CpG-gp-E2 immunization translates to a significant *in vivo* anti-tumor activity toward a self-antigen expressed by an aggressive, poorly immunogenic, syngeneic tumor [51,52]. These important results render the E2 nanoparticle an attractive viral-mimicking platform for further development and optimization to deliver tumor

antigens and adjuvant.

4. Conclusions

We have simultaneously packaged CpG within the interior of the E2 nanoparticle and displayed multiple copies of an MHC I-restricted epitope from the melanocyte differentiation antigen gp100. These multifunctional viral-mimicking E2 particles demonstrated significantly higher *in vitro* CD8⁺ T cell antigen-specific IFN- γ secretion and proliferation. Subcutaneous delivery of CpG within the E2 nanoparticle under the current immunization strategy increased the number of APCs in the local lymph nodes and spleen. Furthermore, the frequency of gp100-specific CD8⁺ T cells in immunized mice was significantly increased by the CpG-gp-E2 nanoparticle formulation, and the CTL response yielded greater tumor cell lysis, compared to control peptide formulations. We have achieved the ability to overcome tolerance to a self TAA, without the need for using live or attenuated pathogens and with a single-dose. Immunization of mice with CpG-gp-E2 nanoparticles followed by challenge with the B16-F10 melanoma tumor line resulted in a significant delay in tumor growth and prolonged life, compared to PBS-treated controls, confirming the anti-tumor capabilities of the antigen-specific CD8⁺ T cells generated with the viral-mimicking E2 formulation. Altogether, this work supports the hypothesis that simultaneous delivery of antigen and immune activator in a virus-mimicking format can enhance cell-mediated anti-tumor antigen responses and, importantly, demonstrates the therapeutic potential of the virus-mimicking E2 nanoparticle as a biomaterial-based vaccine platform for delivering tumor associated antigens.

Acknowledgments

We gratefully acknowledge Dr. Jin Wook Choi and Dr. Javier Cardenas in the laboratory of Prof. Nancy Da Silva for access to and assistance with HPLC, and Prof. Aaron Esser-Kahn for use of his flow cytometer. DLS and mass spectrometry were carried out at the UCI Laser Spectroscopy Facility and the UCI Mass Spectrometry Facility, respectively. We are grateful to Dr. Sergey Ryazantsev at the California NanoSystems Institute at UCLA for assistance with obtaining TEM images. We also thank Dr. Michael Phelan at UCI's Chao Family Comprehensive Cancer Center's Biostatistics Shared Resource Facility for consultation and advice with statistical analyses. This work was supported by the National Institutes of Health (R21EB017995), the National Cancer Institute of the National

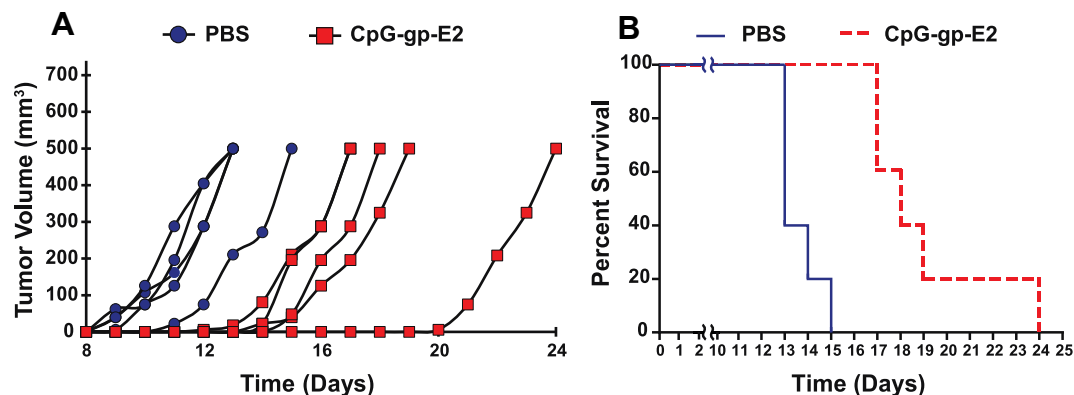


Fig. 7. Immunization with the CpG-gp-E2 nanoparticle delayed B16-F10 tumor growth and increased animal survival time. Data is representative of a duplicate set of independent experiments. Mice ($n = 5$ per group) were immunized subcutaneously with CpG-gp-E2 ($50 \mu\text{g}$ per injection; equivalent to $5 \mu\text{g}$ each of gp100 peptide and CpG ODN) or PBS at Days -28 and -14 , followed by tumor challenge at Day 0. A) Immunization with CpG-gp-E2 exhibited a delayed tumor growth, compared to PBS-treated control. Each line represents the tumor growth of a single animal. B) Immunization with CpG-gp-E2 significantly prolonged animal survival, compared to PBS-treated controls ($p < 0.002$, log-rank test).

Institutes of Health (P30CA062203), and the University of California Cancer Research Coordinating Committee (UCCRC-101868). The content is solely the responsibility of the authors and does not necessarily represent the official views of the National Institutes of Health.

Appendix A. Supplementary data

Supplementary data related to this article can be found at <http://dx.doi.org/10.1016/j.biomaterials.2016.01.056>.

References

- [1] R.D. Schreiber, L.J. Old, M.J. Smyth, Cancer immunoediting: integrating immunity's roles in cancer suppression and promotion, *Science* 331 (2011) 1565–1570.
- [2] C. Guo, M.H. Manjili, J.R. Subjeck, D. Sarkar, P.B. Fisher, X.Y. Wang, Therapeutic cancer vaccines: past, present, and future, *Adv. Cancer Res.* 119 (2013) 421–475.
- [3] S.A. Rosenberg, Decade in review—cancer immunotherapy: entering the mainstream of cancer treatment, *Nat. Rev. Clin. Oncol.* 11 (2014) 630–632.
- [4] C.A. Klebanoff, L. Gattinoni, N.P. Restifo, CD8+ T-cell memory in tumor immunology and immunotherapy, *Immunol. Rev.* 211 (2006) 214–224.
- [5] W.W. Overwijk, M.R. Theoret, S.E. Finkelstein, D.R. Surman, L.A. de Jong, F.A. Vyth-Dreese, et al., Tumor regression and autoimmunity after reversal of a functionally tolerant state of self-reactive CD8+ T cells, *J. Exp. Med.* 198 (2003) 569–580.
- [6] K. Hariharan, G. Braslawsky, A. Black, S. Raychaudhuri, N. Hanna, The induction of cytotoxic T-cells and tumor-regression by soluble-antigen formulation, *Cancer Res.* 55 (1995) 3486–3489.
- [7] C.L. Slingluff Jr., The present and future of peptide vaccines for cancer: single or multiple, long or short, alone or in combination? *Cancer J.* 17 (2011) 343–350.
- [8] C.E. Fadul, J.L. Fisher, T.H. Hampton, E.C. Lallana, Z. Li, J. Gui, et al., Immune response in patients with newly diagnosed glioblastoma multiforme treated with intranodal autologous tumor lysate-dendritic cell vaccination after radiation chemotherapy, *J. Immunother.* 34 (2011) 382–389.
- [9] D.L. Porter, B.L. Levine, M. Kalos, A. Bagg, C.H. June, Chimeric antigen receptor-modified T cells in chronic lymphoid leukemia, *N. Engl. J. Med.* 365 (2011) 725–733.
- [10] S.A. Rosenberg, N.P. Restifo, J.C. Yang, R.A. Morgan, M.E. Dudley, Adoptive cell transfer: a clinical path to effective cancer immunotherapy, *Nat. Rev. Cancer* 8 (2008) 299–308.
- [11] A. Yamada, T. Sasada, M. Noguchi, K. Itoh, Next-generation peptide vaccines for advanced cancer, *Cancer Sci.* 104 (2013) 15–21.
- [12] G.A. Kolumam, S. Thomas, L.J. Thompson, J. Sprent, K. Murali-Krishna, Type I interferons act directly on CD8 T cells to allow clonal expansion and memory formation in response to viral infection, *J. Exp. Med.* 202 (2005) 637–650.
- [13] E.M. Plummer, M. Manchester, Viral nanoparticles and virus-like particles: platforms for contemporary vaccine design, *Wiley Interdiscip. Rev. Nanomedicine Nanobiotechnology* 3 (2011) 174–196.
- [14] F. Steinhagen, T. Kinjo, C. Bode, D.M. Klinman, TLR-based immune adjuvants, *Vaccine* 29 (2011) 3341–3355.
- [15] W.R. Heath, F.R. Carbone, Cross-presentation in viral immunity and self-tolerance, *Nat. Rev. Immunol.* 1 (2001) 126–134.
- [16] J.I. Andorko, K.L. Hess, C.M. Jewell, Harnessing biomaterials to engineer the lymph node microenvironment for immunity or tolerance, *AAPS J.* 17 (2015) 323–338.
- [17] M.F. Bachmann, G.T. Jennings, Vaccine delivery: a matter of size, geometry, kinetics and molecular patterns, *Nat. Rev. Immunol.* 10 (2010) 787–796.
- [18] A. Tan, H. De La Pena, A.M. Seifalian, The application of exosomes as a nanoscale cancer vaccine, *Int. J. Nanomedicine* 5 (2010) 889–900.
- [19] B.D. Lichty, C.J. Breitbach, D.F. Stojdl, J.C. Bell, Going viral with cancer immunotherapy, *Nat. Rev. Cancer* 14 (2014) 559–567.
- [20] Y. Krishnamachari, S.M. Geary, C.D. Lemke, A.K. Salem, Nanoparticle delivery systems in cancer vaccines, *Pharm. Res.* 28 (2011) 215–236.
- [21] N. Kushnir, S.J. Streatfield, V. Yusibov, Virus-like particles as a highly efficient vaccine platform: diversity of targets and production systems and advances in clinical development, *Vaccine* 31 (2012) 58–83.
- [22] D.P. Patterson, A. Rynda-Apple, A.L. Harmsen, A.G. Harmsen, T. Douglas, Biomimetic antigenic nanoparticles elicit controlled protective immune response to influenza, *ACS Nano* 7 (2013) 3036–3044.
- [23] S.M. Goldinger, R. Dummer, P. Baumgaertner, D. Mihic-Probst, K. Schwarz, A. Hammann-Haenni, et al., Nano-particle vaccination combined with TLR-7 and -9 ligands triggers memory and effector CD8(+) T-cell responses in melanoma patients, *Eur. J. Immunol.* 42 (2012) 3049–3061.
- [24] D.R. Ciocca, N. Cayado-Gutierrez, M. Maccioni, F.D. Cuello-Carrion, Heat shock proteins (HSPs) based anti-cancer vaccines, *Curr. Mol. Med.* 12 (2012) 1183–1197.
- [25] S.K. Calderwood, M.A. Stevenson, A. Murshid, Heat shock proteins, autoimmunity, and cancer treatment, *Autoimmun. Dis.* 2012 (2012) 486069.
- [26] M. Dalmau, S. Lim, H.C. Chen, C. Ruiz, S.W. Wang, Thermostability and molecular encapsulation within an engineered caged protein scaffold, *Biotechnol. Bioeng.* 101 (2008) 654–664.
- [27] M. Dalmau, S. Lim, S.W. Wang, Design of a pH-dependent molecular switch in a caged protein platform, *Nano Lett.* 9 (2009) 160–166.
- [28] N.M. Molino, K. Bilotkach, D.A. Fraser, D. Ren, S.W. Wang, Cell uptake and complement responses toward polymer-functionalized protein nanocapsules, *Biomacromolecules* 13 (2012) 974–981.
- [29] D.M. Ren, F. Kratz, S.W. Wang, Protein nanocapsules containing doxorubicin as a pH-responsive delivery system, *Small* 7 (2011) 1051–1060.
- [30] N.M. Molino, A.K. Anderson, E.L. Nelson, S.W. Wang, Biomimetic protein nanoparticles facilitate enhanced dendritic cell activation and cross-presentation, *ACS Nano* 7 (2013) 9743–9752.
- [31] A.F. Kirkin, K. Dzhandzhugazyan, J. Zeuthen, The immunogenic properties of melanoma-associated antigens recognized by cytotoxic T lymphocytes, *Exp. Clin. Immunogenet.* 15 (1998) 19–32.
- [32] X.Y. Wang, X. Chen, M.H. Manjili, E. Repasky, R. Henderson, J.R. Subjeck, Targeted immunotherapy using reconstituted chaperone complexes of heat shock protein 110 and melanoma-associated antigen gp100, *Cancer Res.* 63 (2003) 2553–2560.
- [33] M. Roederer, Interpretation of cellular proliferation data: avoid the panglossian, *Cytom. A* 79 (2011) 95–101.
- [34] D.M. Ren, F. Kratz, S.W. Wang, Engineered drug-protein nanoparticle complexes for folate receptor targeting, *Biochem. Eng. J.* 89 (2014) 33–41.
- [35] S. Goodbourn, L. Didcock, R.E. Randall, Interferons: cell signalling, immune modulation, antiviral response and virus countermeasures, *J. Gen. Virol.* 81 (2000) 2341–2364.
- [36] G.P. Dunn, C.M. Koebel, R.D. Schreiber, Interferons, immunity and cancer immunoediting, *Nat. Rev. Immunol.* 6 (2006) 836–848.
- [37] W. Bohm, S. Thoma, F. Leithauser, P. Moller, R. Schirmbeck, J. Reimann, T cell-mediated, IFN-gamma-facilitated rejection of murine B16 melanomas, *J. Immunol.* 161 (1998) 897–908.
- [38] Z. Zhang, S. Tongchusak, Y. Mizukami, Y.J. Kang, T. Ioji, M. Touma, et al., Induction of anti-tumor cytotoxic T cell responses through PLGA-nanoparticle mediated antigen delivery, *Biomaterials* 32 (2011) 3666–3678.
- [39] J.M. Critchfield, M.K. Racke, J.C. Zunigapflucker, B. Cannella, C.S. Raine, J. Goverman, et al., T-cell deletion in high antigen dose therapy of autoimmune encephalomyelitis, *Science* 263 (1994) 1139–1143.
- [40] W. Jiang, M.M. Lederman, C.V. Harding, B. Rodriguez, R.J. Mohner, S.F. Sieg, TLR9 stimulation drives naive B cells to proliferate and to attain enhanced antigen presenting function, *Eur. J. Immunol.* 37 (2007) 2205–2213.
- [41] R. Edukulla, N. Woller, B. Mundt, S. Knocke, E. Gurlevik, M. Saborowski, et al., Antitumoral immune response by recruitment and expansion of dendritic cells in tumors infected with telomerase-dependent oncolytic viruses, *Cancer Res.* 69 (2009) 1448–1458.
- [42] B. Min, H. Yamane, J. Hu-Li, W.E. Paul, Spontaneous and homeostatic proliferation of CD4 T cells are regulated by different mechanisms, *J. Immunol.* 174 (2005) 6039–6044.
- [43] D. El Kebir, I. Jozsef, W. Pan, L. Wang, J.G. Filep, Bacterial DNA activates endothelial cells and promotes neutrophil adherence through TLR9 signaling, *J. Immunol.* 182 (2009) 4386–4394.
- [44] T. Hara, S. Shitara, K. Imai, H. Miyachi, S. Kitano, H. Yao, et al., Identification of IL-7-producing cells in primary and secondary lymphoid organs using IL-7-gfp knock-in mice, *J. Immunol.* 189 (2012) 1577–1584.
- [45] D.F. Tough, P. Borrow, J. Sprent, Induction of bystander T cell proliferation by viruses and type I interferon in vivo, *Science* 272 (1996) 1947–1950.
- [46] C.W. Lawrence, T.J. Braciale, Activation, differentiation, and migration of naive virus-specific CD8+ T cells during pulmonary influenza virus infection, *J. Immunol.* 173 (2004) 1209–1218.
- [47] S.R. Allie, W. Zhang, S. Fuse, E.J. Usherwood, Programmed death 1 regulates development of central memory CD8 T cells after acute viral infection, *J. Immunol.* 186 (2011) 6280–6286.
- [48] S. Hamdy, O. Molavi, Z. Ma, A. Haddadi, A. Alshamsan, Z. Gobti, et al., Co-delivery of cancer-associated antigen and toll-like receptor 4 ligand in PLGA nanoparticles induces potent CD8+ T cell-mediated anti-tumor immunity, *Vaccine* 26 (2008) 5046–5057.
- [49] Z. Xu, S. Ramishetti, Y.C. Tseng, S. Guo, Y. Wang, L. Huang, Multifunctional nanoparticles co-delivering trp2 peptide and CpG adjuvant induce potent cytotoxic T-lymphocyte response against melanoma and its lung metastasis, *J. Control Release* 172 (2013) 259–265.
- [50] M.R. Olson, D.S. McDermott, S.M. Varga, The initial draining lymph node primes the bulk of the CD8 T cell response and influences memory T cell trafficking after a systemic viral infection, *PLoS Pathog.* 8 (2012) e1003054.
- [51] S.E. Finkelstein, D.M. Heimann, C.A. Klebanoff, P.A. Antony, L. Gattinoni, C.S. Hinrichs, et al., Bedside to bench and back again: how animal models are guiding the development of new immunotherapies for cancer, *J. Leukoc. Biol.* 76 (2004) 333–337.
- [52] M. Zoller, IFN-treatment of B16-F1 versus B16-F10: Relative impact on non-adaptive and T-cell-mediated immune defense in metastatic spread, *Clin. Exp. Metastasis* 6 (1988) 411–429.
- [53] T. Storni, C. Ruedl, K. Schwarz, R.A. Schwendener, W.A. Renner, M.F. Bachmann, Nonmethylated CG motifs packaged into virus-like particles induce protective cytotoxic T cell responses in the absence of systemic side effects, *J. Immunol.* 172 (2004) 1777–1785.
- [54] D.E. Speiser, K. Schwarz, P. Baumgaertner, V. Manolova, E. Devevre, W. Sterry, et al., Memory and effector CD8 T cell responses after nanoparticle vaccination of melanoma patients, *J. Immunother.* 33 (2010) 848–858.